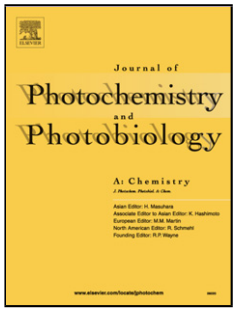

Title: Visible Light Mediated Reductions of Ethers, Amines and Sulfides

Author: Timothy M. Monos Gabriel Magallanes Leanne J. Sebren Corey R.J. Stephenson

PII: S1010-6030(16)30292-1
DOI: http://dx.doi.org/doi:10.1016/j.jphotochem.2016.05.014
Reference: JPC 10233

To appear in: *Journal of Photochemistry and Photobiology A: Chemistry*

Received date: 23-4-2016
Accepted date: 18-5-2016

Please cite this article as: Timothy M.Monos, Gabriel Magallanes, Leanne J.Sebren, Corey R.J.Stephenson, Visible Light Mediated Reductions of Ethers, Amines and Sulfides, Journal of Photochemistry and Photobiology A: Chemistry http://dx.doi.org/10.1016/j.jphotochem.2016.05.014

Visible Light Mediated Reductions of Ethers, Amines and Sulfides

Timothy M. Monos, Gabriel Magallanes, Leanne J. Sebren, Prof. Corey R. J. Stephenson

Department of Chemistry, University of Michigan, Ann Arbor, 48109, USA

Highlights

- Method for the reduction of α–keto ethers amines and sulfides at room temperature using visible light and an Ir(III) photocatalyst.
- Reactions run in ethanol with minimal additive loadings.
- Lignin model substrates containing the β–O–4 motif were reduced in fair to good yields.

Abstract

Visible light-mediated photoredox catalysis enables the chemoselective reduction of activated carbon–heteroatom bonds as a function of reduction potential. The expansion of the scope of C–X bond reductions towards less activated motifs, such as ethers, amines and sulfides, is important to both organic synthesis and macromolecular degradation method development. In the present report, exploration of photoredox catalysis in alcoholic solvents mediated a decrease in the super-stoichiometric use of $^{i}Pr_2NEt$ and HCO_2H in the reduction of α–keto ethers, amines and sulfides. Additionally, in the absence of fragmentation, C–C bond formation was afforded, suggesting an intermediate ketyl radicals are present in these transformations.

1. Introduction

Photoredox catalysis has emerged as a premier method for selective radical generation by single electron transfer (SET) [1]. In this mode of catalysis, reactivity is enabled through the photophysical excitation of a metal or organic dye photosensitizer, which can subsequently participate in bimolecular electron transfer in the excited state [2]. Visible light mediated photocatalysis has mitigated the hazards and environmental incompatibility of radical chemistry conducted with tin reagents and organic radical initiators [3]. While a number of functionalities have been reduced using photoredox catalysis [1], reductions of less labile carbon–heteroatom bonds – including ethers, amines and sulfides – are less prevalent in the literature. These motifs comprise a large portion of organic functional groups, and as such, represent a challenging goal to engage for applications in small molecule synthesis and macromolecular degradation.

One such macromolecule that can benefit from the development of reduction chemistry is lignin. This biopolymer comprises about 30-40% of plant biomass, and is largely discarded as a waste product in the paper pulping industry due to the irregular aryl ether polymeric composition that is highly resistant to chemical degradation [4]. Recently, methods utilizing homogenous transition metal catalysis for the activation of the C–O bonds in lignin biomass have been described [5]. Yet, identifying scalable, chemically efficient reactions for the selective depolymerization of lignin into valuable aromatic products remains the central challenge of emerging technologies.

Recently, we disclosed an approach leveraging photoredox catalysis for the chemoselective reduction of the most prominent polymeric linkage in lignin, the β–O–4 motif (**Figure 1, A-B**) [6]. This protocol consisted of a stoichiometric oxidation followed by a photocatalytic reduction to selectively cleave the β–O–4 bond in a number of model lignin substrates. This method was selective in the presence of γ–hydroxy groups as well as unprotected phenols. Based upon the current mechanistic understanding of ketyl chemistry, we proposed a mechanism for the photoredox reductive cleavage (**Figure 1**) whereby a ketone

substrate (**1**) is first reduced by an Ir(II) species generated from a reductive quenching event with a tertiary amine. Fragmentation of **2** about the C_α–O (**red**) bond affords an acetophenone radical and, after protonation, guaiacol (**4**). Finally, the acetophenone radical can be reduced by an H-atom transfer process [7].

Despite the success of this reaction, the super-stoichiometric use of $^{i}Pr_2NEt$ and HCO_2H was thought to be a prohibiting factor in developing scale-up applications. In this report, we describe our advancements in understanding the photochemical degradation of model lignin substrates, as well as describe the adaptation of this reductive cleavage method for α–keto amines and sulfides (**Figure 1**, **C**).

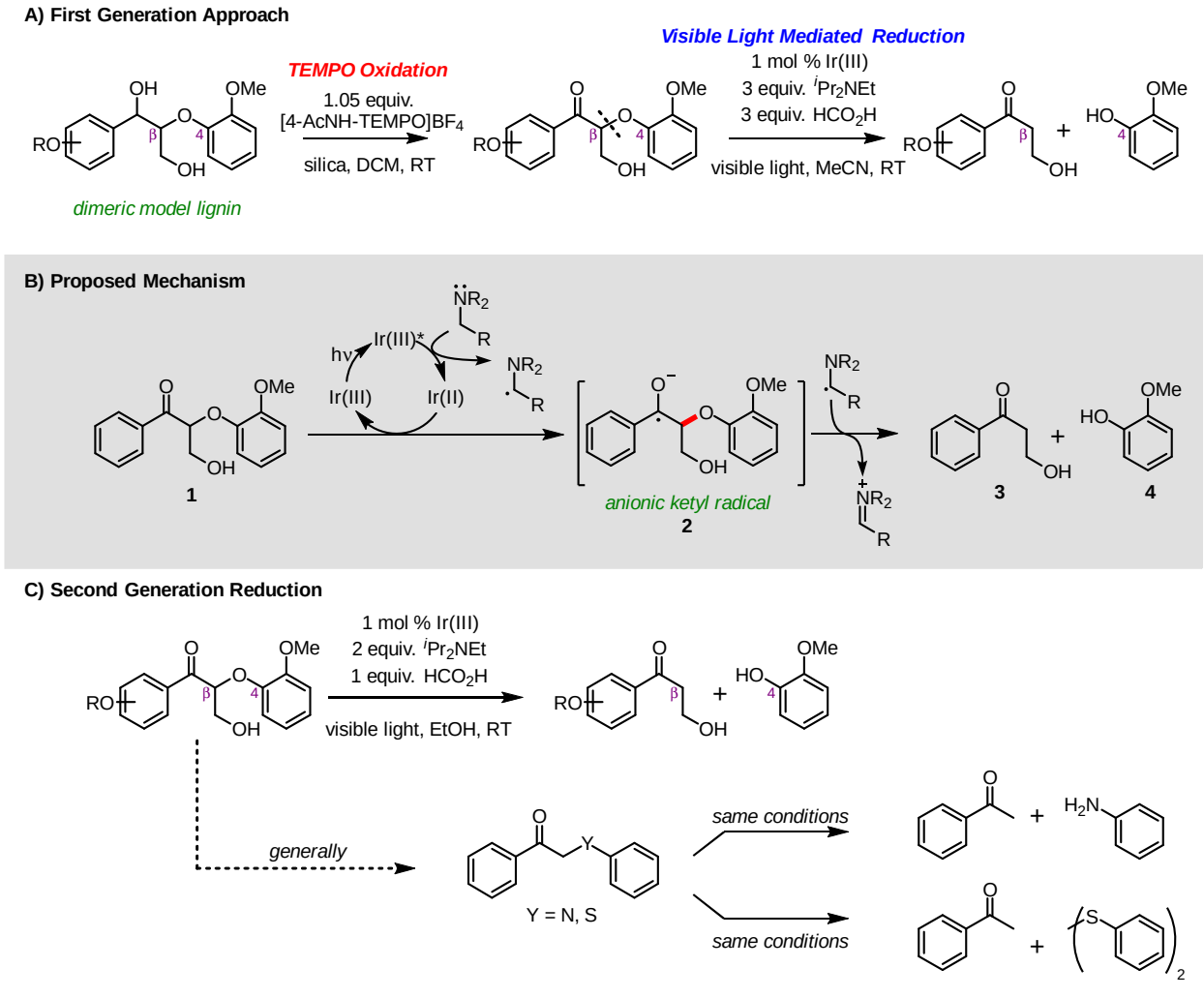

Figure 1: Ketone Reduction-Fragmentation Aproach for α–heteroatom cleavage.

2. Results and Discussion

2.1 Reaction design:

In order to affect the reduction of unstrained C–O, C–N and C–S bonds, we targeted a reduction-fragmentation approach. Previous reports suggested the direct reduction of C_{sp3}–O bonds (E_{red} = –2.23 V vs. SCE [8]) is thermodynamically unfavorable using Ir(III) or Ru(II) based photocatalysts, thus a method targeting an initial carbonyl reduction (E_{red} = –2.10 vs SCE [9]) seemed more feasible. This approach has been meaningfully demonstrated by Molander, with Sm(II) reductants [10], followed by Hasegawa [11] and Olivier [12] with photoredox catalysts (**Figure 2**). For both Molander and Hasegawa, the effective reductants were very reducing and, as a result, engaged aliphatic ketones to afford fragmentation products in high yields. More recently, Olivier's example demonstrated phenyl ketone substituted aziridines are privileged substrates for photoredox catalysis to induce fragmentation. Inspired by these reports, single electron transfer catalyzed by Ir(II) reductants provided similar reactivity in the β–O–4 lignin substrates (**1**) which contained an unstrained α–keto ether motif (**Figure 1**). In this case, the reaction efficiency correlated well with the pK_a of the fragmenting group, and this methodology was effective for model lignin substrates in which the fragmenting group was guaiacol (**4**).

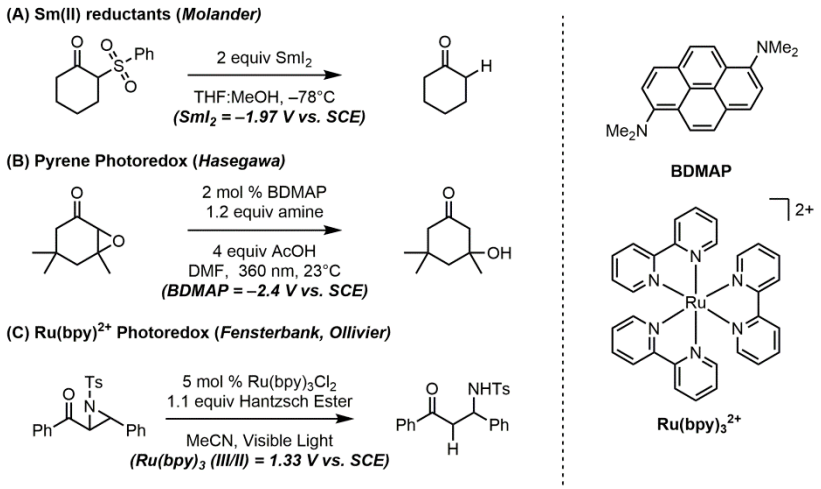

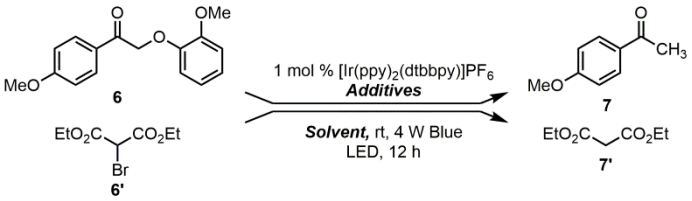

Entry	Substrate	Additive	Solvent	Yield* (isolated)
1	6'	none	MeOH	5%
2	6'	none	EtOH	67%
3	6'	none	^{i}PrOH	46%
4	6'	none	THF	57%
5	6	none	EtOH	0%
6	6	$^{i}Pr_2NEt$ (50 mol %)	EtOH	37%
7	6	$^{i}Pr_2NEt$ (1 equiv)	EtOH	50%
8	6	$^{i}Pr_2NEt$ (2 equiv)	EtOH	82%
9	6	$^{i}Pr_2NEt$ (2 equiv) HCO_2H (1 equiv)	EtOH	100% (72%)
10	6	guaiacol (1 mol %)	EtOH	0%
11	6	guaiacol (100 mol %)	EtOH	0%
12	6	no photocatalyst	EtOH	0%
13	6	no light	EtOH	0%

* yield quantified by GC-MS

In order to address the excess of terminal reductant additives, we targeted using alcoholic solvents for an additional function of terminal H-atom donors [13]. An initial screening of alcoholic and ether solvents as H-atom donors revealed ethanol as a competent solvent in the debromination of diethylbromomalonate [14] (**Figure 3, entries 1-4**). Despite observing good conversions of diethylbromomalonate, the reduction of model lignin **6** failed to convert under the same reaction conditions (**Figure 3, entry 5**). This could be overcome by the addition of $^{i}Pr_2NEt$; yet complete consumption of starting material was not observed in a 12-hour reaction period (**Figure 3, entry 6-8**). Additional time did not reveal further starting material consumption. Upon the addition of formic acid, full consumption of the starting material in 12 hours was observed. Taken together, these results suggested the reductive quenching cycle which engaged the amine as the electron and H-atom source was the most prominent process; however, the use of ethanol could promote the reductive fragmentation of **6**, likely by facilitating Brønsted acid activation better than in acetonitrile did in the first generation conditions. Additionally, Brønsted acid activation by weakly acidic guaiacol did not promote reactivity in the same manner as formic acid. Lastly, control experiments proved light and photocatalyst were necessary for this transformation [14].

2.2 Reaction Scope

The optimized conditions (**Figure 3, entry 11**) proved effective in the reductive fragmentation of model lignin substrates **8**, **9**, and **10** (**Table 1**). While the measured reduction potentials of each of these substrates were nearly identical, –1.77 V vs. SCE [9b], full consumption of **8**, **9**, and **10** occurred over

different reaction times – **8** reduced in 24 hours, **9** in 48 and **10** in 60 hours. This suggested that the overall fragmentation process was kinetically favored in the least alkoxy substituted aryl ketone substrates. Isolation of the reduced lignin fragments (**8a**, **9a**, **10a**) was afforded in moderate to low yield, suggesting the required reaction time for full starting material consumption was also allowing for additional product reactivity and degradation.* Interestingly, substrate **11**, was isolated in high yield, implicating the β–hydroxy motif of **8**, **9** and **10**, to be a promoter of further reactivity. More broadly, this protocol was effective in fragmenting benzyloxyacetaldehyde (**12**) and chalcone epoxide (**13**). The reduction of **12** was only possible in acetonitrile solvent; we speculate this reactivity difference is due to the formation of an acetal of **12** in the alcoholic solvents.

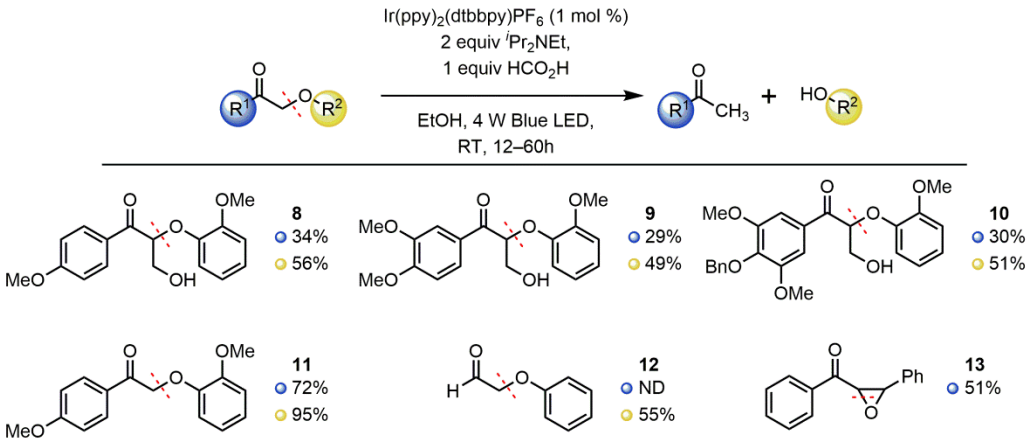

Table 1 Substrate Scope of Ether Reduction

While investigating a broader reduction scope, the developed reaction conditions reduced α–keto amines in good yields (

Table 2). Substrates **17** and **18** converted quickly (6-12 hours) to the fragmented products, while substrate **16** needed a significantly longer reaction time (>24 hours). In addition to amines, α–keto sulfides were efficiently reduced without prior oxidation to sulfoxides or sulfones. In these reductions, the sulfur fragment was isolated as the disulfide rather than the mercaptan. One possibility for disulfide formation

* Yields isolated for substrates **8**, **9**, **10** were isolated in 85-90% yield when reacted under the first generation conditions (see Fig 1 (A)).

occurs via fragmentation to generate a thiyl radical and acetophenone enolate, whereby two thiyl radicals combine to form a disulfide. Additionally, similar to the ether and amine reductions, an anionic thiophenol species could be generated which later participates in a separate oxidation event to afford the disulfide species. Importantly, neither thiophenol nor disulfide mediated α–heteroatom fragmentations were observed as a background reaction.

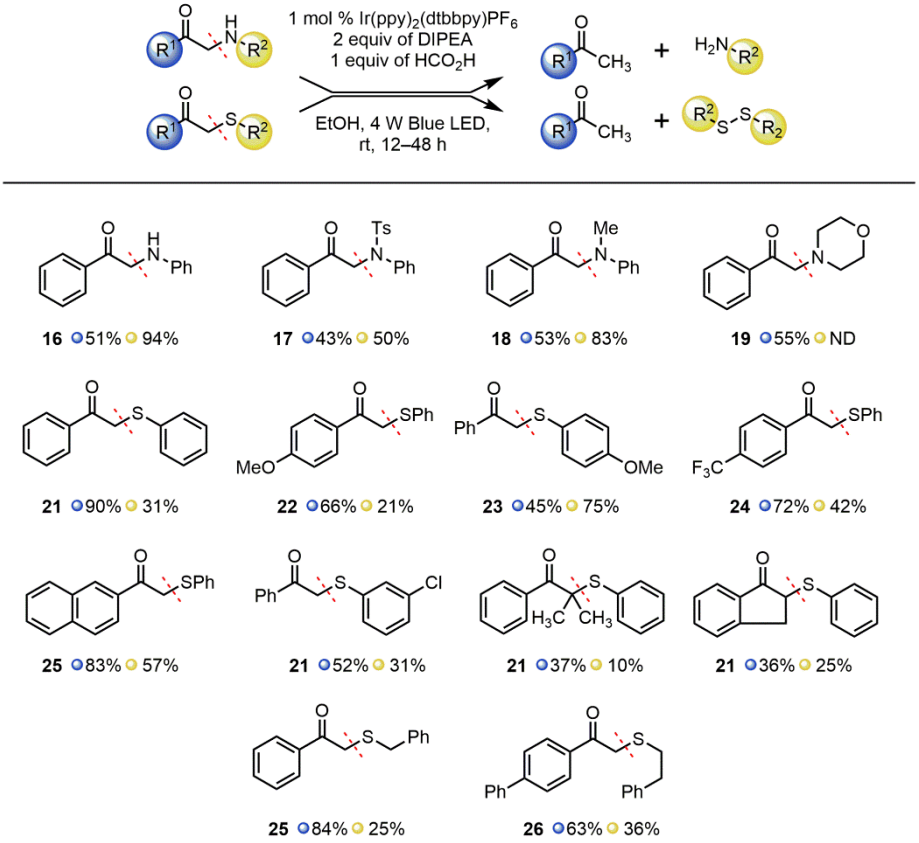

Table 2: Substrate Scope of Amine and Sulfide Reductions

Overall, sulfide substrates containing electron-withdrawing arene substituents (**24**-**26**) fragmented efficiently, to afford moderate to good yields of the reduction products. Conversely, substrates **21**-**23** were sluggish to reduce, but cleanly afforded the fragmentation products. Substrates **27** and **28** were the slowest to reduce, and did not fully convert after reacting for more than 48 hours. Lastly, in contrast to the equivalent ether and amine substrates, the alkyl sulfides (**29**, **30**) cleanly fragmented without any detected pinacol product formation. Substrate **30** was sensitive to the addition of formic acid, but cleanly

fragmented with only 1 equivalent of $^{i}Pr_2NEt$. These results highlight that efficient reductive cleavage of α–keto sulfides can be achieved through photoredox catalysis.

In addition to the observed fragmentation reactivity, selected substrates exhibited pinacol coupling exclusively. This was first observed for substrates **14** and **15** (**Table 3**)**,** whereby the products **14a** and **15a** were afforded in low yields. Reactivity for fragmentation or pinacol coupling is hypothesized to be due to the stability of the intermediate ketyl species balanced with the electronic influence of both the phenyl and oxygen substituents (**Figure 4**). For substrates **8-11**, fragmentation products were afforded as guaiacol is weakly basic and a good leaving group. Substrates **13-15** contain α–hydroxy or alky-ether substituents which disfavor fragmentation from the ketyl intermediate due to the higher basicity of the alcohol fragments. With this slow fragmentation step, the ketyl intermediate can be stabilized by the protic solvent, allowing for a lifetime long enough to form the pinacol products. The apparent outlier of this trend, substrate **12**, fragments because the intermediate ketyl species is too unstable and forces fragmentation before pinacol coupling can occur. Importantly, the fragmentation of **12** was only possible in acetonitrile; fragmentation was not observed in ethanol as the diethylacetal was hypothesized to prevent reactivity. Overall, similar ketyl C–C bond forming processes have been demonstrated by Knowles [15] and Rueping [16], whereby the C–C bond formation is affected by an initial single electron reduction of a phenyl ketone or aldehyde.

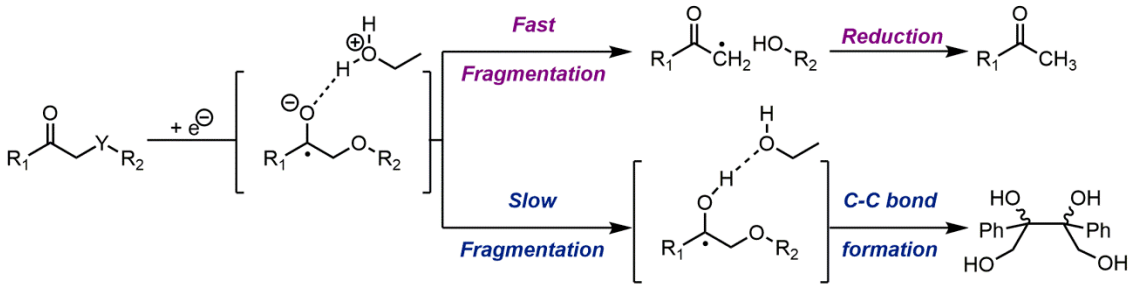

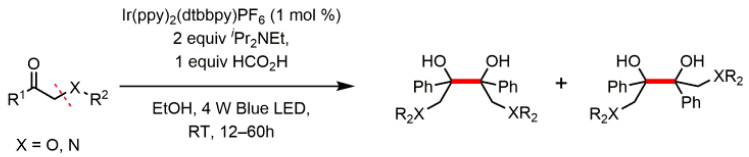

Substrate	Products
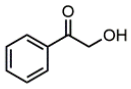 **14**	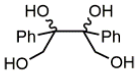 (**14a**) 11% *mixture of isomers*
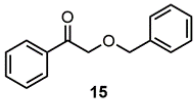 **15**	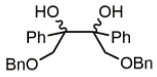 (**15a**) 31% *mixture of isomers*
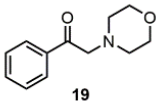 **19**	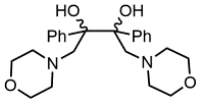 (**19c**) 68% *mixture of isomers* **MeCN solvent*
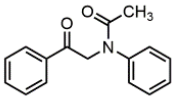 **20**	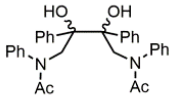 (**20c**) 9% *mixture of isomers*

Table 3: Pinacol Products

3. Conclusions

The continued development of mild and selective carbon–heteroatom bond reductions is critical for both synthesis and biomass conversion processes. Using a Ir(III) photocatalyst, we have demonstrated the reduction of a variety of unstrained α–keto ethers, amines and sulfides using decreased amounts of terminal reductants. This demonstrates progress towards the minimization of reagent stoichiometry, one of the implicit goals of catalytic biomass valorization. Lastly, a radical pathway for C–C bond formation by ketyl dimerization was demonstrated, and appears to be highly influenced by substrate electronics and reaction conditions, both of which we are currently investigating.

4. Experimental

4.1 General Information:

All other chemicals were used as received. Reactions were monitored by TLC and visualized with a dual short wave/long wave UV lamp. Column flash chromatography was performed using 230-400 mesh silica gel or via automated column chromatography. Preparative TLC purifications were run on silica plates of 1000 μm thickness. NMR spectra were recorded on Varian MR400, Varian Inova 500,

Varian Vnmrs 500, or Varian Vnmrs 700 spectrometers. Chemical shifts for ^{1}HNMR were reported as , parts per million, relative to the signal of $CHCl_3$ at 7.27 ppm. Chemical shifts for ^{13}CNMR were reported as , parts per million, relative to the center line signal of the $CDCl_3$ triplet at 77.16 ppm. Chemical shifts for ^{19}FNMR were reported as , parts per million, relative to the signal of a trifluorotoluene internal standard at –63.72 ppm. The abbreviations s, br. s, d, dd, br. d, ddd, t, q, br. q, qi, m, and br. m stand for the resonance multiplicity singlet, broad singlet, doublet, doublet of doublets, broad doublet, doublet of doublet of doublets, triplet, quartet, broad quartet, quintet, multiplet and broad multiplet, respectively. IR spectra were recorded on a Perkin-Elmer Spectrum BX FT-IR spectrometer fitted with an ATR accessory. Mass Spectra were recorded at the Mass Spectrometry Facility at the Department of Chemistry of the University of Michigan in Ann Arbor, MI on an Agilent Q-TOF HPCL-MS with ESI high resolution mass spectrometer. Gas Chromatography yields were run on a Shimadzu GC-MS QP2010 SE with an Rx1 5sil MS column. Yields were calculated based on linear calibration curve of 4-methoxyacetophenone. Electrochemical data was collected on a CHI600E potentiostat with the accompanying CH Instruments software. LED lights and the requisite power box and cables were purchased from Creative Lighting Solutions (http://www.creativelightings.com) with the following item codes: CL-FRS5050-12WP-12V (4.4W blue LED light strip), CL-FRS5050WPDD-5M- 12V-BL (72 W LED strip), CL-PS94670-25W (25 W power supply), CL-PS16020-150W (150 W power supply), CL-PC6FT-PCW (power cord), CL-TERMBL-5P (terminal block).

Unless stated otherwise, all reactions were run on a 1.0 mmol scale in a 2 or 4 dram vial equipped with stir bar and cap. One 4w LED strip was wrapped in a circle around the reaction with the reaction about 3-4 inches from the light source. At this distance the temperature of the reactions did not exceed 35 ˚C.

Preparation of Starting Materials:

4.1.1 Phenylethanone Amines: 2-bromoacetophenone (2.0 g, 10.05 mmol) and ethanol (50 mL, 0.2 M in starting material) were added to a dry round botom flask equipped with a magnetic stir bar. Aniline (1.83 mL, 20.10 mmol, 2 eq.) was added drop-wise, as a white precipitant formed immediately upon addition. This was allowed to stir for 3 hours, upon which the solution was filtered, concentrated *in vacuo*, and recrystallized using ethanol.

4.1.1.1 *1-phenyl-2-(phenylamino)ethan-1-one (16)* - **^{1}H NMR** (400 MHz, $CDCl_3$) 8.03 (d, J ≡ 7.3 Hz, 2H), 7.65 (t, J = 7.4 Hz, 1H), 7.53 (t, J = 7.7 Hz, 2H), 7.31 – 7.22 (m, 3H), 6.81 (t, J = 7.6 Hz, 3H), 4.67 (s, 2H). **^{13}C NMR** (176 MHz, $CDCl_3$) 194.98, 146.95, 134.89, 133.86, 129.37, 128.88, 127.75, 117.94, 113.13, 50.41. **IR** (neat) 3410.9, 1686.3, 1601.9, 1508.4, 1444.8, 1356.9, 1321.6, 1261.8, 1219.9, 1178.8, 1147.7, 984,864.4, 743.6, 684.2, 663.5. **HRMS** (*m/z)* – 212.1070 $[M+H]^+$. **R_f** (7:3 Hexanes:EtOAc) = 0.64

4.1.1.2 *4-methy-N-(2-oxo-2-phenylethyl)-N-phenylbenzenesulfonamide (17)* - **^{1}H NMR** (700 MHz, $CDCl_3$) 7.95 (dd, *J* = 8.2, 1.1 Hz, 2H), 7.60 (d, *J* = 7.4 Hz, 1H), 7.59 – 7.55 (m, 2H), 7.47 (t, *J* = 7.8 Hz, 2H), 7.32 – 7.23 (m, 5H (2+3), *overlap with $CHCl_3$*), 7.18 – 7.14 (m, 2H), 5.05 (s, 2H), 2.44 (s, 3H). **^{13}C NMR** (176 MHz, $CDCl_3$) 193.87, 143.86, 139.74, 135.61, 135.06, 133.78, 129.53, 129.22, 128.86, 128.85, 128.39, 128.16, 77.34, , 76.98, 57.78, 21.75. **IR** (neat): 3061.9, 2917.1, 1707.2, 1595.3, 1491.8, 1447.4, 1335.1, 1364.6, 1305.8, 1291.6, 1212.6, 1184.4, 1103.8, 1089.9, 1029.7, 1011.6, 1000.4, 980.1, 881.8, 935.3, 912.4, 809.2, 768.2, 755.0, 768.2, 729.9, 667.0, 692.9 **HRMS** (*m/z)* = 366.1158 [M+H].

4.1.2 Phenylethanone Sulfides: Prepare a solution of thiol and base ethanol solution, 0.2 M with respect to the thiol. Allow for equilibration and cooling for 30 minutes. Separately, prepare a solution of 2-bromoacetophenone in ethanol, and add slowly to the reaction. Allow appropriate time for reaction. Quench the reaction with an equimolar amount of acid, and then precipitate the product by adding a large excess of water. Crude crystals can be recrystallized in MeOH-H_2O.

4.1.2.1 *1-phenyl-2-(phenylthio)ethan-1-one (21)* - **^{1}H NMR** (700 MHz, $CDCl_3$) **7.96** (dd, J = 8.4, 1.2 Hz, 2H), 7.96 (dd, J = 8.4, 1.2 Hz, 2H), 7.60 (ddt, J = 8.6, 7.2, 1.2 Hz, 1H), 7.48 (dd, J = 8.1, 7.4 Hz, 2H), 7.42 –7.38 (m, 2H), 7.32 – 7.28 (m, 2H), 7.26 – 7.21 (m, 1H), 4.29 (s, 2H). **^{13}C NMR** (176 MHz, $CDCl_3$) **133.47,** 130.52, 129.05, 128.67, 128.67, 127.11, 41.2. **HRMS** (m/z) = 229.0682 [M+H]+. **IR** (neat) 3074.1, 1668.8, 1596, 1578.4, 1479.2, 1444.9, 1416.1, 1273.2, 1185.8, 1133.9, 1072.5, 1011.2, 941.7, 898, 804.3, 740.5, 722, 66.6, 648.1, 614.1 Rf (EtOAc/Hexanes (1:5)) = 0.50

4.1.2.2 *1-(4-methoxyphenyl)-2-(phenylthio)ethan-1-one (22)* - **^{1}H NMR** (500 MHz, $CDCl_3$) **7.98** – 7.91 (m, 2H), 7.43 – 7.37 (m, 2H), 7.32 – 7.27 (m, 2H), 7.25 – 7.20 (m, 1H), 6.97 – 6.92 (m, 2H), 4.25 (s, 2H), 3.89 (s, 3H). **^{13}C NMR** (176 MHz, $CDCl_3$) **192.68, 163.76, 135.03,** 131.02, 130.34, 129.00, 128.37, 126.94, 113.83, 55.49, 40.95. **IR** (neat) 1658.2, 1601.4, 1572, 1508.6, 1480.4, 1420.3, 1436.7, 1395.9, 1310.5, 1262.6, 1199.9, 1173.8, 1023.7, 991.6, 817.8, 734.3, 690, 633.1. **HRMS** (m/z) 259.0682 [M+H]+ **R_f** (EtOAc/Hexanes 1:5) 0.55.

4.1.2.3 2-((4-methoxyphenyl)thio)-1-phenylethan-1-one (23)- **^{1}H NMR** (500 MHz, $CDCl_3$) **7.93 (d,** J = 7.8 Hz, 2H), 7.57 (d, J = 7.3 Hz, 1H), 7.47 (t, J = 7.6 Hz, 2H), 7.37 (d, J = 8.6 Hz, 2H), 6.83 (d, J = 8.6 Hz, 2H), 4.14 (s, 2H), 3.80 (s, 3H). **^{13}C NMR** (176 MHz, $CDCl_3$) **194.29 (s),** 159.73 (s), 135.45 (s), 134.65 (s), 133.29 (s), 132.64 (s), 130.48 (s), 128.94 (s), 128.65 (d, J = 18.3 Hz), 126.30 (s), 124.52 (s), 114.82 (s), 114.63 (d, J = 18.7 Hz), 77.18 (s), 76.99 (s), 76.81 (s), 55.29 (s), 42.79 (s). **IR** (neat) 2937.2, 2835.3, 1674.0, 1591.1, 1492.3, 1461.7, 1447.4, 1406.0, 1274.1, 1242.8, 1196.2, 1172.8, 1133.5, 1104.0, 1075.9, 1027.9, 1014.0, 1075.9, 1027.9, 1014.0, 825.8, 798.3, 748.4, 723.8, 686.9. **HRMS** (*m/*z): 259.0788 [M+H]+.

4.1.2.4 *2-(phenylthio)-1-(4-(trifluoromethyl)phenyl)ethan-1-one (24)* - **^{1}H NMR** (700 MHz, $CDCl_3$) 8.04 (d, *J* = 8.1 Hz, 15H), 7.74 (d, *J* = 8.1 Hz, 15H), 7.41 – 7.36 (m, 14H), 7.30 (ddd, *J* = 6.6, 2.4, 0.8 Hz, 14H), 7.28 (t, *J* = 1.3 Hz, 3H), 7.27 – 7.25 (m, 4H), 4.26 (s, 16H). **^{13}C NMR** (176 MHz, $CDCl_3$) **193.18** (s), 138.21(s), 135.08(s), **134.80** (q, *J* = 32.8 Hz), 134.70 (s), 134.52 (s), 134.10 (s), 131.18 (s), 129.35 (s), 129.21 (s), 125.98 (s), 125.88 (q, *J* = 3.7 Hz), 123.65 (q, *J* = 272.7 Hz), 121.33 (s), 41.42 (s). **^{19}F NMR** (471 MHz, $CDCl_3$) ppm = –64.17 (s, 3 F)**.** **IR** (neat) 2896.7, 1679.3, 1580.0, 1511.7, 1482.4, 1438.6, 1409.9, 1393.0, 1326.1, 1311.2, 1311.2, 1285.7, 1195.7, 1162.8, 1111.1, 1065.1, 1026.9, 1015.1, 992.4, 964.0, 900.1, 854.4, 839.0, 825.5, 739.9, 701.1, 689.8. **HRMS (***m/z)* **=** 297.055 $[M+H]^+$. **R_f**(9:1 Hexanes:EtOAc) = 0.36 (stains light green in vanillin)

4.1.2.5 *1-(naphthalen-2-yl)-2-(phenylthio)ethan-1-one (25)* - **^{1}H NMR** (700 MHz, $CDCl_3$) **8.44 (s,** 1H), 8.02 (dd, J = 8.6, 1.6 Hz, 1H), 7.96 – 7.86 (m, 3H), 7.63 (t, J = 7.4 Hz, 1H), 7.57 (t, J = 7.5 Hz, 1H), 7.43 (d, J = 7.5 Hz, 2H), 7.30 (t, J = 7.5 Hz, 2H), 7.25 (t, J = 7.3 Hz, 1H), 4.41 (s, 2H). **^{13}C NMR** (176 MHz, $CDCl_3$) **194.20, 135.86, 134.95, 132.85, 132.56, 130.87,** 130.73, 129.79, 129.25, 128.88, 128.73, 127.94, 127.35, 127.02, 124.36, 41.53. **IR** (neat)

3073.2, 3048.4, 2952.3, 2898.7, 2898.7, 1676.0, 1622.7, 1581.6, 1505.9, 1478.8, 1466.1, 1436.0, 1389.7, 1355.9. 1293.9, 1271.1, 1244.5, 1164.5, 1124.3, 1093.9, 1070.5, 1024.1, 1024.1, 984.5, 972, 944.7, 925.8, 890.3, 864.5, 810.1, 767.9, 748.6, 727.7, 685.7. **HRMS** (*m/z)***:** 301.0658 [M+Na^+]. $\mathbf{R}_f$ (9:1 Hexanes:EtOAc) = 0.32

4.1.2.6 *2-((3-chlorophenyl)thio)-1-phenylethan-1-one (26)* - **^{1}H NMR** (700 MHz, $CDCl_3$) **7.96 (dd,** J = 8.4, 1.2 Hz, 1H), 7.61 (ddd, J = 2.4, 1.8, 1.2 Hz, 1H), 7.52 – 7.47 (m, 1H), 7.38 (t, J = 1.6 Hz, 1H), 7.27 (m, 1 H) *overlap with chloroform*, 7.22 (t, J = 7.5 Hz, 1H), 7.21 – 7.19 (m, 1H), 4.32 (s, 1H). **^{13}C NMR** (126 MHz, $CDCl_3$) **193.72,** 137.10, 135.41, 133.82, 130.21, 129.80, 128.92, 128.80, 128.16, 127.24, 41.02. **IR** (neat) 3052.3, 2943.0, 2913.8, 1686.2, 1593.2, 1573.4, 1561.6, 1561.6, 1464.3, 1445.8, 1404.1, 1382.3, 1382.3, 1322.5, 1308.1, 1288.9, 1196.9, 1180.2, 1116.2, 1086.1, 1086.1, 1077.5, 1026.0, 999.3, 980.0, 884.0, 884, 871.3, 775.7, 765.0, 751.5, 687.0, 680.2. **HRMS** (*m/z):* 263.0292 [M+H^+]. $\boldsymbol{R}_f$ (9:1 Hexanes:EtOAc) = 0.33

4.1.2.7 *((2-fluorophenyl)thio)-1-phenylethan-1-one (27)* - **^{1}H NMR** (700 MHz, $CDCl_3$) 7.96 (dd, J = 8.4, 1.2 Hz, 1H), 7.61 (tt, J = 7.41, 1.21 Hz, 1H), 7.51 – 7.48 (m, 1H), 7.38 (t, J = 1.6 Hz, 1H), 7.27(dt, J = 7.48,1.57 Hz, 1H *overlap with $CDCl_3$*), 7.22 (t, J = 7.5 Hz, 1H), 7.21 – 7.19 (m, 1H) , 4.32 (s, 2H). **^{13}C NMR** (126 MHz, $CDCl_3$) **193.98 (s) 162.17 (d, J ≡ 246.5 Hz), ,** 135.52 (s), 134.05 (s), 134.04 (s), 133.65 (s), 129.96 (d, J = 8.0 Hz), 128.80 (d, J = 9.5 Hz), 124.74 (d, J = 3.8 Hz), 121.33 (d, J = 17.6 Hz), 116.02 (d, J = 22.5 Hz), 40.51 (s). **^{19}F NMR** (471 MHz, $CDCl_3$) -109.06 (ddd, *J* = 9.4, 7.5, 5.5 Hz). **IR** (neat) 3070.3, 2947.6, 2911.4, 1679.9, 1593.5, 1578.8, 1565.6, 1465.8, 1445.9, 1397.5, 1317.6, 1284.4, 1261.9, 1220.1, 1191.4, 1180.6, 1160.0, 1123.1, 1070.2, 1031.3, 999.4, 983.7, 927.8, 888.2, 852.9, 826.9, 806.3, 806.3, 743.3, 687.4, 678.4. **HRMS** (*m/z)* = 269.0407 [M+ Na^+]. $\mathbf{R}_f$ (9:1 Hexanes:EtOAc) = 0.40

4.1.2.8 *2-methyl-1-phenyl-2-(phenylthio)propan-1-one (28)* - **^{1}H NMR** (700 MHz, $CDCl_3$) **8.25 (d,** J = 8.4 Hz, 2H), 7.54 (td, J = 7.7, 1.0 Hz, 1H), 7.46 (t, J = 7.7 Hz, 2H), 7.38 – 7.32 (m, 3H), 7.32 – 7.24 (m, 2H, *overlap with $CHCl_3$*), 1.57 (s, 6H). **^{13}C NMR** (176 MHz, $CDCl_3$) **201.20** (s), 137.90 (s), 137.16 (s), 132.49 (s), 131.78 (s), 130.48 (s), 130.16 (s), 129.59 (s), 128.84 (s), 55.67 (s), 27.59 (s). **IR** (neat) : 3060.3, 2967.4, 2928.0, 1665.8, 1595.6, 1574.2, 1473.5, 1460.9, 1438.7, 1383.5, 1364.5, 1304.0, 1259.7, 1157.3, 1118.8, 1088.3, 1068.0, 1024.9, 1002.0, 975.5, 881.6, 792.4, 750.0, 732.1, 702.2. **HRMS** (*m/z)* = 257.0994 [M+H^+] $\mathbf{R}_f$(9.5:0.5 Hexanes:EtOAc) = 0.42

4.1.2.9 *2-(phenylthio)-2,3-dihydro-1H-inden-1-one (29)* - **^{1}H NMR** (700 MHz, $CDCl_3$) **ppm 3.13** (dd, *J*=17.54, 3.75 Hz, 8 H) 3.63 (dd, *J*=17.71, 7.66 Hz, 9 H) 4.08 (dd, *J*=7.83, 3.75 Hz, 8 H) 7.21 - 7.30 (m, 29 H) 7.34 - 7.42 (m, 15 H) 7.44 - 7.52 (m, 15 H) 7.54 - 7.67 (m, 9 H) 7.78 (d, *J*=7.66 Hz, 7 H). **^{13}C NMR** (176 MHz, $CDCl_3$) **ppm 34.79,** 50.34, 124.58, 126.29, 127.12, 127.46, 127.67, 127.84, 128.95, 132.30, 133.28, 135.26, 135.43, 152.06, 202.23. **IR** (neat) 3058.7, 2906.7, 1763.5, 1721.7, 1602.1, 1580.3, 1602.1, 1580.3, 1481.7, 1470.7, 1437.9, 1419.7, 1325.4, 1299.4, 1273.8, 1205.8, 1185.6, 1173.6, 1146.0, 1087.8, 1020.8, 1008.1, 957.1, 892.4, 849.7, 792.9, 780.4, 740.6, 729.8, 711.0, 689.5. **HRMS (*m/z)*** = 241.0682 [M+H^+] $\mathbf{R}_f$ (9:1 Hexanes:EtOAc)= 0.46

4.1.2.102-(benzylthio)-1-phenylethan-1-one (30) - **^{1}H NMR** (500 MHz, $CDCl_3$) **ppm 3.67 (s, 2 H)** 3.76 (s, 2 H) 7.17 - 7.28 (m, 2 H) 7.32 (t, *J*=7.46 Hz, 2 H) 7.34 - 7.38 (m, 2 H) 7.43 - 7.49 (m, 2 H) 7.52 - 7.60 (m, 1 H) 7.93 (d, *J*=8.07 Hz, 2 H) **^{13}C NMR** (176 MHz, $CDCl_3$): **194.40**, 137.26, 135.36, 133.32, 129.26, 128.68, 128.64, 128.52, 127.22, 36.06, 35.82. **IR** (neat):

1670.2, 1595.7, 1449.8, 1394.7, 1292.3, 1197.4, 998.8, 751.1, 685.3, 638.4, 552.6, 536.0, 526.3, 497.6, 480.1, 447.3, 417.9, 412.5. **HRMS** (*m/z*) = 265.0658 [M+Na^+].

4.1.2.11 *1-([1,1'-biphenyl]-4-yl)-2-(phenethylthio)ethan-1-one (31)*- **^{1}H NMR** (700 MHz, $CDCl_3$) ppm ^{1}H NMR (700 MHz, $CDCl_3$) **8.06 (d, J ≡ 8.4 Hz, 2H), 7.70 (d, J ≡ 8.4 Hz, 2H), 7.64** (dd, J = 8.2, 1.1 Hz, 2H), 7.49 (t, J = 7.7 Hz, 2H), 7.42 (t, J = 7.4 Hz, 1H), 7.30 (dd, J = 9.5, 5.7 Hz, 2H), 7.22 (dd, J = 7.2, 5.3 Hz, 3H), 3.84 (s, 2H), 2.93 (dd, J = 8.9, 6.4 Hz, 2H), 2.89 – 2.83 (m, 2H). **^{13}C NMR** (176 MHz, $CDCl_3$) **ppm 13C NMR (176 MHz, cdcl3) 194.16 (s),** 146.22 (s), 140.22 (s), 139.95 (s), 133.96 (s), 129.55 (s), 129.12 (s), 128.73 (s), 128.63 (s), 128.45 (s), 127.48 (s), 127.43 (s), 126.57 (s), 37.20 (s), 35.72 (s), 33.79 (s). **IR** (neat): 2914.2, 2139.9, 2183.1, 2172.7, 2066.2, 1977.0, 2017.31971.9, 1955.0, 1660.3, 1599.9, 1560.5, 1485.1, 1452.8, 1419.8, 1310.9, 1288.9, 1270.1, 1204.5, 1139.5, 1159.9, 1072.8, 1034.3, 1002.6, 927.7 855.8, 845.8, 714.5, 698.5, 988.2, 647.5, 633.9, 609.3, 615.0, 620.1, 604.0 **HRMS** (*m/z*) = 333.1308 [M+H^+]. **R_f** (9:1 Hexanes:EtOAc): 0.55 (brown in anisaldehdye stain).

4.2 General Reaction Procedure:

Phenyl ketone (0.50 mmol – 1.0 mmol) was added to a round bottom or 4 dram vial with ^{i}Pr_2NEt (2 equiv.), HCO_2H (1 equiv.) and photocatalyst [Ir(ppy)$_2$(dtbbpy)PF_6] (1 mol %). These reactants were diluted in EtOH (5 mL, 0.20 M in starting material), and irradiated by 1x4W Blue LED strip until reaction completion (6-96 hours). At this point the ethanol was removed *in vacuo*, and the resulting oil was diluted in water and extracted with ethyl acetate. The organic portion was washed with 4 N $HCl_{(aq)}$, saturated sodium bicarbonate solution, brine and finally dried with Na_2SO_4, after which it was concentrated to an oil. If the starting material contained acetophenone as the phenacyl fragment, 1 eq. of PhTMS was added to the oil and the mixture was diluted in $CDCl_3$. This was analyzed via ^{1}H NMR to obtain an accurate acetophenone yield. If the starting material yields an acetophenone derivative heavier than acetophenone, then the PhTMS standardization step was omitted. After which the crude reaction was purified by SiO_2 chromatography to afford the fragmentation products.

4.2.1 *2,3-diphenylbutane-1,2,3,4-tetraol (14c)* - **^{1}H NMR** (500 MHz, $CDCl_3$) (1.4:1 racemic:meso) **7.38** – 7.28 (m, 3H), 7.26 – 7.16 (m, 3H), 6.99 (bs 1H), 6.98 (bs, 1H), 4.22 (d, J = 11.7 Hz, 1H), 3.98 (dd, J = 28.3, 11.8 Hz, 2 H), 3.52 (d, J = 11.8 Hz, 1H). **^{13}C NMR** (126 MHz, $CDCl_3$) **140.53, 139.45, 128.03, 127.82, 127.71, 127.62, 127.23, 127.10, 80.25, 79.55,** 66.47, 66.32. **IR** (neat): 3379.4, 2946.3, 2246.0, 1956.1, 1601.2, 1492.5, 1446.3, 1384.2, 1184.8, 1119.3, 1066.0, 1051.7, 953.3, 906.8, 841.5, 761.8, 729.1, 702.4, 645.0, 620.8, 611.2. HRMS (m/z) = 292.2268

4.2.2 *1,4-bis(benzyloxy)-2,3-diphenylbutane-2,3-diol (15c)* - **^{1}H NMR** (500 MHz, $CDCl_3$) **7.35** – 7.28 (m, 3H), 7.26 – 7.18 (m, 5H), 7.17 – 7.12 (m, 2H), 4.42 (q, J = 11.9 Hz, 2H), 4.05 (d, J = 9.7 Hz, 1H), 3.89 (s, 1H), 3.77 (t, J = 12.6 Hz, 1H). **^{13}C NMR** (176 MHz, $CDCl_3$) **141.27,** 137.77, 128.48, 127.97, 127.88, 127.38, 127.18, 127.03, 79.30, 74.71, 73.77. **IR**(neat) = 3548.0, 1495.1, 1446.3, 1403.8, 1359.9, 1301.6, 1252.2, 1208.2, 1127.6, 1101.4, 1066.4,

1048.8, 1034.2, 914.6, 818.6, 738.5, 703.1, 616.3, 600.2, 582.1, 558.8, 545.1, 536.3, 528.8, 512.9, 505.8, 501.9, 487.1, 480.3, 46739, 452.7, 445.7. **HRMS** (*m/z*) = 477.2036 [M+Na^+]

4.2.3 *N,N'-(2,3-dihydroxy-2,3-diphenylbutane-1,4-diyl)bis(N-phenylacetamide) (20c)* - ^{1}H NMR (700 MHz, $(CD_3)_2SO$) [**meso:racemic (1:2)**] **7.22 (t,** *J* = 7.1 Hz, 2H), 7.19 (t, *J* = 7.0 Hz, 2H), 7.17 – 7.13 (m, 2H), 6.88 (t, *J* = 7.1 Hz, 1H), 6.60 (s, 1H), 6.43 (s, 2H), 4.95 (d, *J* = 14.5 Hz, 1H), 4.39 – 4.30 (m, 1H), 3.95 (d, *J* = 14.6 Hz, 2H), 3.82 (d, *J* = 14.6 Hz, 2H), 1.59 (s, 3H), 1.46 (s, 6H). **^{13}C NMR** (126 MHz, $(CD_3)_2SO$) **185.51, 185.34, 174.61, 174.36, 174.31,** 144.71, 142.07, 141.67, 129.26, 127.90, 127.75, 127.62, 127.37, 127.00, 126.55, 126.21, 87.38, 82.15, 81.14, 58.31, 58.10, 22.98, 22.75. **IR** (neat): 3224.1 (broad OH), 3054.6, 1624.9, 1591.9, 1494.4, 1443.5, 1397.8, 1354.1, 1298.4, 1241.3, 1176.1, 1116.6,1068.4, 1019.7, 784.0, 741.2, 884.0, 843.8, 765.9, 746.8, 726.1, 695.8, 635.5, 623.9, 608.7, 558.9, 551.9, 526.6, 502.4, 491.2, 484.4, 477.9, 467.4, 449.3, 436.4, 421.3, 411.3. **HRMS** (*m/z*) = 509.2435 [M+H^+].

4.2.4 *1-(4-(benzyloxy)-3,5-dimethoxyphenyl)-3-hydroxypropan-1-one (10a):* ^{1}H NMR (500 MHz, $CDCl_3$): δ 7.47 (d, J = 7.2 Hz, 2H), 7.36-7.29 (m, 3H), 7.21 (s, 2H), 5.12 (s, 2H), 4.04 (t, J=5.3 Hz, 2H), 3.89 (s, 6H), 3.21 (t, J=5.3 Hz, 2H**). ^{13}C NMR (126 MHz, $CDCl_3$)** = 199.45, 153.62, 141.98, 137.40, 132.21, 128.57, 128.37, 128.22, 105.75, 75.18, 58.38, 56.47. **IR (neat)** 2929.3, 1675.1, 1585.9, 1455.0, 1413.9, 1320.5, 1157.6, 1126.7, 700.9 **HRMS (m/z)** = 317.1381 $[M+1]^+$ **R_f:** 0.21 (7:3 EtOAc:Hexanes)

5. Acknowledgements

Financial support from the National Science Foundation (CHE-1440118), the Camille and Henry Dreyfus Foundation, and the University of Michigan is gratefully acknowledged. We thank Dr. John D. Nguyen, Dr. Bryan Matsuura, Dr. Märkus Kärkäs, Dr. Verner Lofstrand, Dr. Daryl Staveness, Joel Beatty and Mitchell Keylor for their helpful discussions.

6. References

[1] **For photoredox catalysis reviews:** (a) J.M.R. Narayanam, C.R.J. Stephenson, Visible light photoredox catalysis: applications in organic synthesis, Chem. Soc. Rev. 40 (2010) 102–113. doi:10.1039/B913880N.(b) J.W. Tucker, C.R.J. Stephenson, Shining Light on Photoredox Catalysis: Theory and Synthetic Applications, J. Org. Chem. 77 (2012) 1617–1622. doi:10.1021/jo202538x. (c) C.K. Prier, D.A. Rankic, D.W.C. MacMillan, Visible Light Photoredox Catalysis with Transition Metal Complexes: Applications in Organic Synthesis, Chem. Rev. 113 (2013) 5322–5363. doi:10.1021/cr300503r. (d) Y. Xi, H. Yi, A. Lei, Synthetic applications of photoredox catalysis with visible light, Org. Biomol. Chem. 11 (2013) 2387–2403. doi:10.1039/C3OB40137E. (e) D.P. Hari, B. König, Synthetic applications of eosin Y in photoredox catalysis, Chem. Commun. 50 (2014) 6688–6699. doi:10.1039/C4CC00751D. (f) R.A. Angnes, Z. Li, C.R.D. Correia, G.B. Hammond, Recent synthetic additions to the visible light photoredox catalysis toolbox, Org. Biomol. Chem. 13 (2015) 9152–9167. doi:10.1039/C5OB01349F. (g) D.A. Nicewicz, T.M. Nguyen, Recent Applications of Organic Dyes as Photoredox Catalysts in Organic Synthesis, ACS Catal. 4 (2014) 355–360. doi:10.1021/cs400956a.

[2] (a) A. Juris, V. Balzani, F. Barigelletti, S. Campagna, P. Belser, A. von Zelewsky, Ru(II) polypyridine complexes: photophysics, photochemistry, eletrochemistry, and chemiluminescence, Coord. Chem. Rev. 84 (1988) 85–277. doi:10.1016/0010-8545(88)80032-8. (b) V. Balzani, S. Campagna A. Meijere, K.N. Houk, H. Kessler, S.V. Ley, J.-M. Lehn, et al., Photochemistry and Photophysics of Coordination Compounds II, Springer-Verlag Berlin Heidelberg, 2007.

[3] W.P. Neumann, Tri-n-butyltin Hydride as Reagent in Organic Synthesis, Synthesis. (1987) 665–683. doi:10.1055/s-1987-28044.

[4] J. Zakzeski, P.C.A. Bruijnincx, A.L. Jongerius, B.M. Weckhuysen, The Catalytic Valorization of Lignin for the Production of Renewable Chemicals, Chem. Rev. 110 (2010) 3552–3599. doi:10.1021/cr900354u.

[5] (a) M. D. Kärkäs , B. S. Matsuura, T. M. Monos, G. Magallanes, C.R.J. Stephenson, Transition-metal catalyzed valorization of lignin: the key to a sustainable carbon neutral future, Org. Biomol. Chem. (2016) doi: 0.1039/C5OB02212F (b) P.J. Duess, J. Barta, J.G. de Vries, Homogeneous catalysis for the conversion of biomass and biomass-derived platform chemicals, Catal. Sci. Technol.;4 (2014), 1174-1196.

[6] J.D. Nguyen, B.S. Matsuura, C.R.J. Stephenson, A Photochemical Strategy for Lignin Degradation at Room Temperature, J. Am. Chem. Soc. 136 (2014) 1218–1221. doi:10.1021/ja4113462.

[7] J.W. Beatty, C.R.J. Stephenson, Amine Functionalization via Oxidative Photoredox Catalysis: Methodology Development and Complex Molecule Synthesis, Acc. Chem. Res. 48 (2015) 1474–1484. doi:10.1021/acs.accounts.5b00068.

[8] The original measurement was –2.27 to –2.34 V. Experimental conditions: epoxide [0.005 M] in DMF, [0.1] M Bu_4NClO_4, reference electrode 0.1 M Ag/AgI/0.1M I^-, hanging mercury drop working electrode. AgI→Ag + I^- = –0.152 vs. SHE. K. Boujlel, J. Simonet, Cathodic Cleavage of Carbon-Oxygen Bonds (V). Direct and Indirect Electrochemical Reduction of Epoxides, Electrochimica Acta., 1979, 24, 481–487. doi:10.1016/0013-4686(79)85020-3.

[9] The original measurement reported was –2.10 V vs. SCE. Experimental conditions: 0.1 M tetraethylammonium perchlorate supporting electrolyte in acetonitrile at 20 °C. Ag/AgCl (–0.042 V vs SCE) reference electrode, mercury hanging drop working electrode. (a) F. M. Martens, J.W. Verhoeven, R.A. Gase, U.K. Pandit, Th. H. deB, oer, On the Question of One-Electron Transfer in the Mechanism of Reduction by NADH-Models, Tetrahedron, 1978, 34, 4, 443-446. (b) Fukuzumi, K. Ishikawa, K. Hironaka, T. Tanaka, Acid catalysis in thermal and photoinduced electron-transfer reactions, J. Chem. Soc. Perkin Trans. 2. (1987) 751–760. doi:10.1039/P29870000751. (b) see supporting information for independently measured reduction potentials of substrates.

[10] G.A. Molander, G. Hahn, Lanthanides in organic synthesis. 2. Reduction of α–heterosubstituted ketones, J. Org. Chem. 51 (1986) 1135–1138. doi:10.1021/jo00357a040. (b) E_{red} describes the reduction half- potential measured in THF, and recalculated from E_{red}= –1.41 V vs. Fe^+/Fe in THF: (c)R.J. Enemærke, K. Daasbjerg, T. Skrydstrup, Is Samarium diiodide an inner- or outer-sphere electron donating agent? Chem. Commun. 1999, 343-344. (d) N.G. Connelly, W.E. Hahn, Chemical Redox Agents for Organometallic Chemistry, Chem. Rev. 1996, 887-910.

[11]E. Hasegawa, S. Takizawa, T. Seida, A. Yamaguchi, N. Yamaguchi, N. Chiba, et al., Photoinduced electron-transfer systems consisting of electron-donating pyrenes or anthracenes and benzimidazolines for reductive transformation of carbonyl compounds, Tetrahedron. 62 (2006) 6581–6588. doi:10.1016/j.tet.2006.03.061. (b) E_{red} describes the reduction half-potential based on a direct oxidative quench between photoexcited BDMAP* and a ketone substrate in acetonitrile.

[12] M.-H. Larraufie, R. Pellet, L. Fensterbank, J.-P. Goddard, E. Lacôte, M. Malacria, et al., Visible-Light-Induced Photoreductive Generation of Radicals from Epoxides and Aziridines, Angew. Chem. Int. Ed. 50 (2011) 4463–4466. doi:10.1002/anie.201007571. (b) E_{red} describes the reduction half-potential from Ru(II) to Ru(III) in acetonitrile.

[13] (a) Amatore, C.; Badoz-Lambling, J.; Bonnel-Huyghes, C.; Pinson, J.; Savaént, J.M.; Thiébault, A.; J. Am. Chem. Soc., 1982, 104, 1979-1986 (b) Andrieux, C.P.; Badoz-Lambling, J.; Combellas, C.; Lacombe, D.; Savaént, J.M.; Thiébault, A.; Zann, D.; J. Am. Chem. Soc., 1987, 109, 1518-1525 (c) Bordwell, F. G.; Zhang, X.; Alnajjar, M. S. J. Am. Chem. Soc. 1992, 114 (20), 7623–7629. (d) Alfassi, Z. B.; Golden, D. M. J. Phys. Chem. 1972, 76 (23), 3314–3319. (e) S. Mizuta, S. Verhoog, K.M. Engle, T. Khotavivattana, M. O'Duill, K. Wheelhouse, et al., Catalytic Hydrotrifluoromethylation of Unactivated Alkenes, J. Am. Chem. Soc. 135 (2013) 2505–2508. (f) W.J. Boyle, J.F. Bunnett, Relative reactivities of methanol and methoxide ion as hydrogen atom donors to the p-nitrophenyl radical, J. Am. Chem. Soc. 96 (1974) 1418–1422.

[14] See supporting information for details.

[15] (a) L.J. Rono, H.G. Yayla, D.Y. Wang, M.F. Armstrong, R.R. Knowles, Enantioselective Photoredo,, x Catalysis Enabled by Proton-Coupled Electron Transfer: Development of an Asymmetric Aza-Pinacol Cyclization, J. Am. Chem. Soc. 135 (2013) 17735–17738. doi:10.1021/ja4100595. (b) K.T. Tarantino, P. Liu, R.R. Knowles, Catalytic Ketyl-Olefin Cyclizations Enabled by Proton-Coupled Electron Transfer, J. Am. Chem. Soc. 135 (2013) 10022–10025. doi:10.1021/ja404342j.

[16] M. Nakajima, E. Fava, S. Loescher, Z. Jiang, M. Rueping, Photoredox-Catalyzed Reductive Coupling of Aldehydes, Ketones, and Imines with Visible Light, Angew. Chem. Int. Ed. 54 (2015) 8828–8832. doi:10.1002/anie.201501556.